PHYSICAL REVIEW A **69**, 041603(R) (2004)

Observation of superradiant Raman scattering in a Bose-Einstein condensate

Yutaka Yoshikawa,* Toshiaki Sugiura, Yoshio Torii, and Takahiro Kuga
Institute of Physics, University of Tokyo, 3-8-1 Komaba, Meguro-ku, Tokyo 153-8902, Japan
(Received 11 November 2003; published 22 April 2004)

We observed superradiant Raman scattering from a Bose-Einstein condensate irradiated by a single off-resonant light beam. Spontaneous mode selection of the scattered radiation turns probabilistic optical pumping into a stimulated Raman process, whereby the atoms are coherently transferred into a different hyperfine state. The population in the pumped state grew exponentially in time, demonstrating the emergence of bosonic stimulation in the optical pumping process.

DOI: 10.1103/PhysRevA.69.041603 PACS number(s): 03.75.−b, 32.80.−t, 42.50.Gy

The coherent interaction between light and collective atoms in a single quantum state has been widely studied following the realization of Bose-Einstein condensation in dilute atomic vapors [1–6]. When the condensate is exposed to a single, off-resonant light beam (pump beam), a strong correlation between successive Rayleigh scattering events emerges because of its high degree of coherence. This results in highly directional emissions of light and recoiling beams of the atoms, referred to as superradiant Rayleigh scattering [1–3]. The growth process of the emitted light and recoiling atoms is known as bosonic stimulation in four-wave mixing of optical and matter waves [2]. This has been interpreted as a self-amplified diffraction from the matter-wave grating formed by the condensate and recoiling atoms [1]. While this picture facilitates an intuitive understanding of the physical process, the fundamental question remains whether the density-grating formation is essential for superradiance in the condensate.

In 1954, Dicke predicted an emergence of coherence in spontaneous emission from an excited atomic ensemble [7]. The degree of coherence is maximum when all the dipole moments oscillate in phase. This is referred to as the maximum cooperative state, corresponding to the condensate "dressed" by the pump beam [1–6]. However, Dicke's treatment can be applied to a variety of atomic systems without introducing the concept of density grating. Likewise, Fermi's golden rule, which gives the light-scattering rate in the first-order perturbation [2], leads to bosonic stimulation as long as energy and momentum conservation is fulfilled. An important factor is the coherence between the initial and final states of atoms or photons, and thus, superradiance is expected for not only the Rayleigh process but also the Raman process, corresponding to nondegenerate four-wave mixing of light and atoms.

In this Rapid Communication, we report the observation of superradiant Raman scattering in Rubidium (Rb) condensates prepared in the upper hyperfine $F=2$ state, from which the recoiling atoms are pumped into the lower hyperfine $F=1$ state. This optical pumping process is originally an incoherent, probabilistic population transfer [8] that changes to a fully coherent process for the condensate due to bosonic stimulation under certain experimental conditions. The concept of the "matter-wave grating" becomes obscure in this case, since the initial and final states of atoms are different quantum states and no density modulation is formed.

Two experimental conditions are required to demonstrate the superradiant Raman scattering. The probability of Raman scattering into a particular Zeeman sublevel in the $F=1$ state must be greater than that of any other transitions. This is imperative because the number of atoms in the most populated sublevel is preferentially amplified by bosonic stimulation. In addition, the spontaneous emission pattern must have a finite mode component propagating toward a long axis of the condensate, along which the superradiant gain is maximum (this scattered mode is known as the "end-fire mode") [3].

To fulfill these conditions, we chose specific energy levels and an experimental geometry, as illustrated in Fig. 1. The Rb condensate is first produced in the $|F,m_F\rangle=|2,2\rangle$ hyperfine ground state in a magnetic trap, and driven by a single pump beam linearly polarized along the z axis and applied from the y direction [Fig. 1(a)]. This π-polarized pump beam induces the $\Delta m_F=0$ transitions by taking the quantization axis along the z axis, which is equal to the long axis of the condensate and the bias-field direction of the magnetic trap. When its frequency is tuned nearly to the D_1 line (the wavelength $\lambda=795$ nm), the atoms are excited only via the $|2,2\rangle\rightarrow|2,2\rangle'$ transition within the dipole selection rule [Fig. 1(b)], where the kets $|\cdots\rangle$ and $|\cdots\rangle'$ stand for the electronic

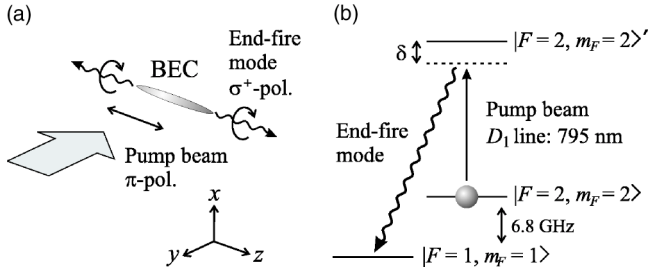

FIG. 1. (a) Geometry and (b) energy-level diagram of the experiment. The condensate of ^{87}Rb atoms is first produced in the $|F,m_F\rangle=|2,2\rangle$ state and pumped into the $|1,1\rangle$ state via the stimulated Raman process between the π-polarized pump beam and σ^+-polarized end-fire mode. The quantization axis is assumed to be the z axis.

*Electronic address: yutaka@phys.c.u-tokyo.ac.jp

ground and excited states, respectively. While the excited $|2,2\rangle'$ state has three decay pathways to the $|2,2\rangle$, $|2,1\rangle$, and $|1,1\rangle$ states, the $|2,2\rangle' \rightarrow |1,1\rangle$ transition has the largest dipole moment corresponding to the branching ratio $1/2$ (those to the $|2,2\rangle$ and $|2,1\rangle$ states are $1/3$ and $1/6$, respectively). Notice that the rate of Raman scattering is the greatest in this configuration and that the superradiant Rayleigh scattering is suppressed. Decay into the $|1,1\rangle$ state changes the magnetic quantum number by $\Delta m_F = -1$, and the spontaneous emission pattern should be $(3/4\pi)\cos^2\theta_j$, where θ_j is the angle between the z axis and the light-emission direction. The intensity is maximum along the z axis ($\theta_j = 0$), and the end-fire modes can therefore be efficiently amplified [Fig. 1(a)]. In the previous study with the sodium condensate in the $|1,-1\rangle$ state and the pump beam tuned around the D_2 transition [1], the branching ratio into the original $|1,-1\rangle$ state was always the largest for both parallel and perpendicular polarizations, and thus superradiant Raman scattering tends to be suppressed.

In contrast, when the polarization of the pump beam is perpendicular to the elongated condensate, the σ^- transitions coupled to the $|2,1\rangle'$ and $|1,1\rangle'$ states are excited. The most probable decay under these conditions is into the original $|2,2\rangle$ state, and normal superradiant Rayleigh scattering then occurs.

The detailed experimental procedure was as follows. We first produced a Rb condensate containing $N_{F,k} = N_{2,0} = 1.7 \times 10^6$ atoms in a magnetic trap. The subscripts F and k represent the hyperfine state and wave vector of the atoms, respectively. The Thomas-Fermi radii of the condensate were about $d_r = 7$ μm along the radial direction and $d_z = 85$ μm along the axial direction. The condensate was then exposed to a pump beam of an intensity $I_p = 230$ mW/cm^2 and a diameter ~ 5 mm for a variable duration Δt. The optical frequency ω_0 was set several gigahertz lower than the $F=2 \rightarrow F'=2$ transition frequency ω_A (the detuning $\delta = \omega_0 - \omega_A < 0$). The magnetic trap was turned off immediately after the pump beam pulse, and velocity distributions of the atoms in the $F=2$ or $F=1$ state were measured independently after a ballistic expansion. To observe the $F=2$ atoms, we used a simple absorption imaging technique with a 10 μs probe pulse resonant with the $F=2 \rightarrow F'=3$ transition of the D_2 line. For imaging of the $F=1$ atoms, we added two operations to the above procedure: We applied a "blower" beam with the same frequency as the probe beam immediately after the pump beam to blow away the remaining atoms in the $F=2$ state. Its intensity was 2 mW/cm^2 and the duration was 16 μs. The atoms in the $F=1$ state were less affected by the blower beam, and, just before the absorption imaging, pumped back into the $F=2$ state by a weak repumping beam tuned to the D_2 line: $F=1 \rightarrow F'=2$ transition.

Figures 2(a) and 2(b) indicate the predicted recoiling patterns for the perpendicular (x-) and parallel (z-) polarized pump beams, respectively, and (c)–(f) depict the experimental results for $\delta = 2\pi \times -2.6$ GHz and $\Delta t = 100$ μs. The perpendicular polarization led to normal superradiant Rayleigh scattering as shown in (c), where the produced momentum side modes propagating along 45° with respect to the pump beam are clearly observed. On the other hand, a negligible population in the $F=1$ state in (e) indicates the suppression

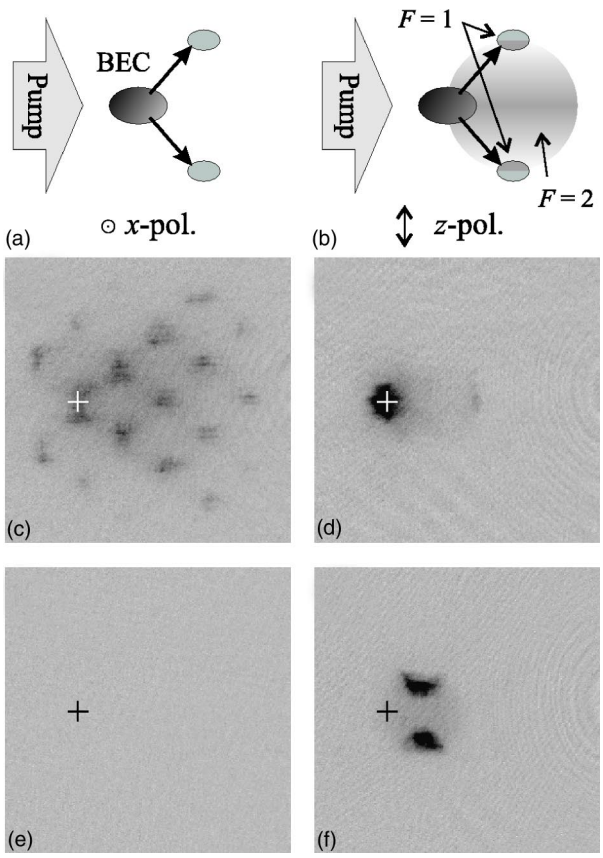

FIG. 2. Schematic diagrams of the superradiant scattering for (a) perpendicular polarization and (b) parallel polarization. Observed density distributions after 25 ms time of flight in the $F=2$ ($F=1$) states are shown in (c) [(e)] for perpendicular polarization, and in (d) [(f)] for parallel polarization. Cross marks in the images indicate the center position of the original condensate. The field of view of these images is 1 mm $\times$ 1 mm.

of incoherent hyperfine pumping during stimulated light scattering in the $F=2$ state [9]. The backward peaks in the $F=2$ state were generated by Raman-Nath (Kapitza-Dirac) diffraction from the optical standing waves formed by the pump and end-fire modes [4]. This phenomenon is energetically allowed only in the early phases during which the uncertainty of the photon energy $\sim \hbar/\Delta t$ exceeds the recoil energy of the atoms, $\hbar\omega_r$. The above condition is satisfied within $\Delta t \simeq 10$ μs for the Rb atoms.

For the parallel polarization, the $F=2$ atoms formed the normal dipole emission pattern barely visible in (d). It was very similar to the result presented in Ref. [1]. However, a major difference was found in the $F=1$ state, where the superradiant Raman scattering created first-order side modes, as shown in (f). Although we cannot identify the Zeeman sublevel of these atoms from this image, they were strongly accelerated and fell more quickly than free fall when we kept the magnetic trap turned on after the formation of the side modes. This indicates that the internal state of the side modes was surely the $|1,1\rangle$ state, since it was strong-field seeking for the magnetic field.

In contrast to (c), we found that higher-order side modes never appeared, even if the parameters of the pump beam

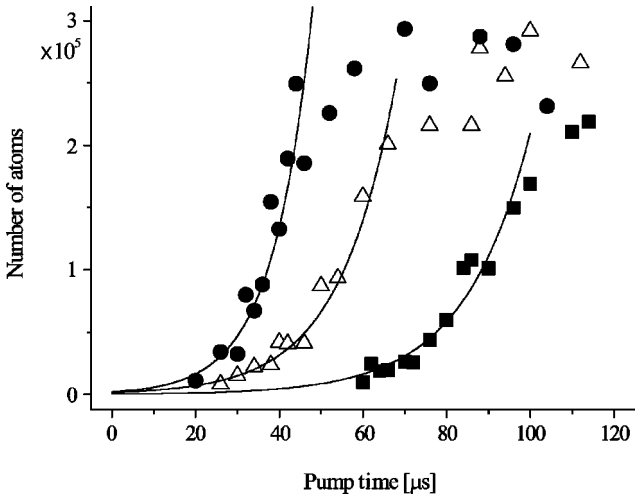

FIG. 3. Number of atoms in the $F=1$ state per peak plotted as the duration of the pump beam. The pump intensity was 230 mW/cm^2. The black circles, white triangles, and black squares correspond to $\delta/(2\pi)=-2.3$, -2.9, and -3.5 GHz, respectively. Solid lines are exponential fits to the initial rise of the respective data.

were varied. This was because, once atoms are pumped into the $|1,1\rangle$ state, an increase of δ by hyperfine splitting between the ground states $\Delta\omega_{hf}=2\pi\times 6.8$ GHz and parallel polarization of the pump beam prohibits subsequent superradiance in the $|1,1\rangle$ state. Furthermore, this frequency difference strongly prevented Raman-Nath diffraction producing the backward atoms, since the Raman-Nath condition in this experiment was approximately given as $\Delta t<1/\Delta\omega_{hf}$ ~ 20 ps, which is six orders of magnitude shorter than in Rayleigh scattering. In fact, no difference was found compared with the long-pulse case shown in (d) and (f) even when we shortened $\Delta t=4$ μs and decreased δ to $2\pi\times -0.5$ GHz to keep the number of light scattering events almost constant.

We measured the evolution of the population in the $|1,1\rangle$ state by changing Δt to study the pumping process more quantitatively. Figure 3 illustrates the obtained population per side mode for several detunings, i.e., for several pumping rates. The solid lines represent exponential fits to the initial part of each data set and show good agreement with the observed steep rises. This exponential growth clearly indicates an emergence of bosonic stimulation in the optical pumping process. It is fully probabilistic at an early stage and gives recoil momentum to atoms in various directions. However, once the end-fire modes become dominant, incoherent optical pumping is switched to stimulated Raman transition, by which a photon in the pump beam is absorbed and stimulated to be emitted into the end-fire mode. The emitted photon and produced coherence between the recoiling and stationary atoms further enhance the subsequent Raman-scattering rate, and the end-fire modes and $|1,1\rangle$ atoms are then self-amplified in pairs.

This interpretation can be formulated by a semiclassical calculation based on the optical Bloch equation [2,6]. The (quasi-)steady-state transition rate of a stimulated Raman process for a weak end-fire mode can be written as

$$W_B = N_{2,0}\Omega_R \,\mathrm{Im}(\rho_{12}) \sim \frac{N_{2,0}\Omega_R^2}{\Gamma_d}, \tag{1}$$

where Ω_R is the two-photon Rabi frequency induced by the pump beam and end-fire mode, ρ_{12} is the off-diagonal density matrix elements of the $|1,1\rangle$ and $|2,2\rangle$ states, and Γ_d is the decoherence rate of the Raman process. Substituting the expression $\Omega_R^2=3\gamma R\lambda^2\Gamma_d n_e/(2\pi A)$ [6] into Eq. (1) yields the following rate equation for the $F=1$ side mode $N_{1,q}$ with momentum $\hbar q=\sqrt{2}\hbar k_0$ [4]:

$$\dot{N}_{1,q} = \frac{3}{2\pi}\frac{\lambda^2}{A}\gamma R N_{2,0} N_{1,q}, \tag{2}$$

where $A\sim\pi d_r^2$ is the cross section of the condensate, γ is the branching ratio into the $|1,1\rangle$ state, and R is the single-atom excitation rate for the $|2,2\rangle\rightarrow|2,2\rangle'$ transition. We have assumed here that the number of photons in the end-fire mode n_e is identical to $N_{1,q}$ produced within the coherence time $1/\Gamma_d$ [2,4]. Equation (2) leads to exponential growth of $N_{1,q}$ for a weak pumping regime $N_{2,0}\gg N_{1,q}\gg 1$ with the rate constant $G=3\lambda^2\gamma R N_{2,0}/(2\pi A)$ [10].

A fully quantum-mechanical treatment also gives the same result when we apply the assumption $n_e=N_{1,q}$ introduced above. Fermi's golden rule gives the net rate of the superradiance as $W_F\propto N_{2,0}(N_{1,q}+n_e+1)$, which can be replaced by $N_{2,0}(2N_{1,q}+1)$. The factor 2 of $N_{1,q}$ represents merely an equivalence of $N_{1,q}$ and n_e, and does not mean the bosonic stimulation by both the optical and atomic final states [it should be expressed by the multiplied form $N_{2,0}(N_{1,q}+1)(n_e+1)$]. More precisely, the growth equation for the general momentum state is given as

$$\dot{N}_{1,j} = \frac{3\cos^2\theta_j}{4\pi}\gamma R\Omega_j N_{2,0}(2N_{1,j}+1), \tag{3}$$

where Ω_j is the phase-matching solid angle for emitted photons [1,3]. Assuming Raman scattering into the end-fire modes $\Omega_j\sim\lambda^2/A$, $\theta_j=0$, and $N_{1,j}\gg 1$ results in the same equation as Eq. (2). In addition, a summation of Eq. (3) over all jth states for $N_{1,j}\ll 1$ describes spontaneous optical pumping correctly, i.e., $\Sigma_j\dot{N}_{1,j}=\gamma R N_{2,0}$.

The experimentally obtained growth rate G is plotted versus the total optical pumping rate $\gamma R N_{2,0}$ in Fig. 4. The vertical and transversal error bars originate from the uncertainty of the exponential fit and determination of R and $N_{2,0}$, respectively. A linear fit to the data gives the geometrical factor of the superradiance $3\lambda^2/(2\pi A)$ of $(6.0\pm 0.8)\times 10^{-4}$, which represents the probability that the pump photons are spontaneously scattered into the end-fire mode at the beginning of superradiance. On the other hand, the condensate radius $d_r=7.0\pm 0.5$ μm yields the theoretical value $(2.0\pm 0.3)\times 10^{-3}$, which is several times greater than the experimental value. The cause of this discrepancy can be attributed to the uncertainty of the definition of A or Ω_j, and the effect of decoherence of the Raman process [10].

Formally, there is no fundamental difference between Rayleigh and Raman superradiance. The problem is how to interpret ρ_{12} in Eq. (1). In the Rayleigh-scattering case, ρ_{12}

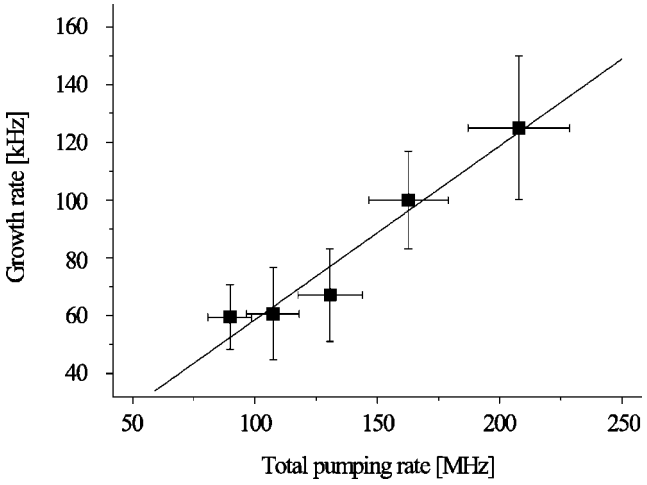

FIG. 4. Growth rate G vs total optical pumping rate $\gamma R N_{2,0}$. Solid line is a linear fit with a gradient of $(6.0\pm0.8)\times10^{-4}$, which represents the geometrical factor of the superradiance.

represents the amplitude of density modulation formed by two atomic motional states [3,6], whereas it is regarded in our experiment as the simply hyperfine coherence between the $|2,2\rangle$ and $|1,1\rangle$ atoms.

However, a decoherence mechanism of two processes would be practically different. In the Rayleigh scattering, Γ_d is mainly determined by the spatial overlap time of two matter-wave fields (transit-time broadening) [5], and any external field does not lead to decoherence since both initial and final internal states are the same. In contrast, for Raman scattering, the field fluctuation and inhomogeneity can cause severer decoherence than the transit-time broadening. For example, a magnetic inhomogeneity of the trapping potential 10 mG over the condensate (assumed to be the curvature 100 G/cm^2) leads to 44 kHz decoherence rate, which is about ten times grater than the case of Rayleigh scattering [1,5].

In conclusion, we observed superradiant Raman scattering in a Bose-Einstein condensate for a particular experimental condition. High degree of coherence of the condensate turned spontaneous Raman scattering into stimulated process, by which atoms were "coherently" pumped into a different hyperfine state. The number of optically pumped atoms grew exponentially in time, exhibiting an emergence of bosonic stimulation in an otherwise probabilistic process.

This work was supported by Grants in Aid for Scientific Research from MEXT, the Matsuo Foundation, and the Mitsubishi Foundation.

[1] S. Inouye, A. P. Chikkatur, D. M. Stamper-Kurn, J. Stenger, D. E. Pritchard, and W. Ketterle, Science **285**, 571 (1999).

[2] W. Ketterle and S. Inouye, in *Bose-Einstein Condensates and Atom Lasers*, edited by A. Aspect and J. Dalibard, Comptes Rendus de l'Académie des Science Paris Vol. IV (Elsevier, Paris, 2001), pp. 339–380.

[3] M. G. Moore and P. Meystre, Phys. Rev. Lett. **83**, 5202 (1999).

[4] D. Schneble, Y. Torii, M. Boyd, E. W. Streed, D. E. Prichard, and W. Ketterle, Science **300**, 475 (2003).

[5] J. Stenger, S. Inouye, A. P. Chikkatur, D. M. Stamper-Kurn, D. E. Pritchard, and W. Ketterle, Phys. Rev. Lett. **82**, 4569 (1999).

[6] S. Inouye, R. F. Löw, S. Gupta, T. Pfau, A. Görlitz, T. L. Gustavson, D. E. Pritchard, and W. Ketterle, Phys. Rev. Lett. **85**, 4225 (2000).

[7] R. H. Dicke, Phys. Rev. **93**, 99 (1954).

[8] See, for example, W. Happer, Rev. Mod. Phys. **44**, 169 (1972).

[9] From the Clebsch-Gordan coefficients, we can estimate the spontaneous pumping probability into the $|1,-1\rangle$ and $|1,0\rangle$ states to be about 25 % in total. However, we could not find any atoms in Fig. 2(e).

[10] In the actual system, the loss term $-\Gamma_d N_{1,q}$ must be added to Eq. (2), and the net growth rate is given by $G-\Gamma_d$. However, in the present study, we ignored the loss term for simplicity.